Incremental adaptive networks implemented by free space optical (FSO) communication

Amir Aminfar, M. Chehel Amirani, Ch. Ghobadi
Department of Electrical and Computer Engineering, Urmia university, Urmia-Iran,
a.aminfar@urmia.ac.ir, m.amirani@urmia.ac.ir, ch.ghobadi@urmia.ac.ir
Corresponding author Email: a.aminfar@urmia.ac.ir

***Abstract*—The aim of this paper is to fully analyze the effects of free space optical (FSO) communication links on the estimation performance of the adaptive incremental networks. The FSO links in this paper are described with two turbulence models namely the Log-normal and Gamma-Gamma distributions. In order to investigate the impact of these models we produced the link coefficients using these distributions and assumed that the network is exchanging data between the nodes that are contaminated with these coefficients. Firstly, by the FSO link assumption, we performed the theoretical analysis for the steady-state performance of the adaptive network and driven closed-form relations explaining the link impacts. Secondly, we performed simulation results for Log-normal and Gamma-Gamma link conditions and presented various results for different levels of turbulence. Finally, we compared the theoretical and analytical results showing a close agreement between these two findings. The results are presented by the means of mean square deviation (MSD) and excess mean square error (EMSE) values.**

Index Terms— *FSO links, adaptive networks, incremental LMS (ILMS), distributed strategies, Log-normal and Gamma-Gamma distributions.*

I. INTRODUCTION

The incremental adaptive networks are the first distributed strategies that have been introduced to overcome the deficiencies of the centralized networks [1, 2]. These networks need the lowest amount of communication between nodes and therefore the lowest amount of communication in order to estimate a desired value. The performance of incremental networks first has been analyzed with ideal radio frequency (RF) links in [2] and [3]. Then, in [4], these networks have been considered with noisy links. It has been shown that the noisy link, which is a practical assumption in real-world applications, can degrade the performance of networks. Next in [1] these networks have been considered in fading channel conditions. The famous Rayleigh fading channel has been introduced to the incremental networks and the link coefficients between nodes have been assumed to follow the Rayleigh distribution. In recent years, however, the advancement of free space optical (FSO) communication appliances, that use visible light rays instead of radio waves, made this technology applicable to almost all communication systems. Wireless sensor networks and their specific relative

Manuscript received 11-June-2018 and revised 14-August-2018,
Accepted on 8- Sept.-2018
P- ISSN: 2322-4088
E- ISSN: 2322-3936

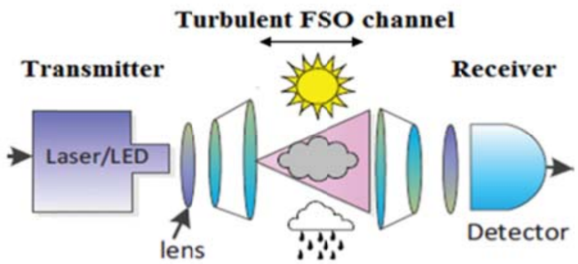

Fig. 1. Free space optical communication through turbulent channel.

adaptive networks are one important branch of these systems that can be implemented using visible light communication.

In analyzing the physical layer for the wireless sensor networks, investigating the accurate performance of these networks in different channel types and conditions is the most important branch of research and numerous researchers have worked in this area to clarify the exact performance of adaptive networks. As we mentioned, the RF links between nodes in adaptive networks have the problem of noise and fading, but the channels in FSO communication systems suffer from a different kind of disturbance namely the channel turbulence. The exact cause of channel turbulence is the change in refractive index of light in free space which is due to the variations in the environment such as fog, rain, dust etc. (see Fig. 1).

Now, we consider the advantages and the disadvantages of both RF and FSO systems. The FSO system has unregulated bandwidth while the bandwidth for RF communication needs licensing because a majority of spectrum parts for this system are occupied. Also, the equipment for RF systems is more bulky and expensive in comparison with the FSO system equipment. Both systems are affected by weather conditions. However, FSO communication is far more secure than RF communication. For these reasons, we considered the implementation of adaptive networks using FSO communication. In Fig. 2, we depicted an adaptive incremental network implemented with FSO or RF communication links.

The implementation of wireless sensor networks with FSO and visible light communication technology is a confirmed branch of science [12]. In most of the FSO implemented systems, the security and the unregistered bandwidth merits are mentioned [17, 20 and 21]. Also, the fact that the radio waves are cancerous is a problem that makes the use of visible light waves more interesting. However, the line of sight and turbulent environments are the problems that we try to overcome. Usually, the line of sight is not a problem for wireless sensor networks implemented in open areas.

However, working through FSO links must be analyzed in detail for adaptive networks and this is the contribution of this paper. We emphasize that none of the references in this paper mentioned the implementation of adaptive incremental networks with the FSO technology. The FSO channel modeling is considered in many references for communication systems other than sensor networks including [6]. The FSO channel noise is usually considered to be Additive White Gaussian Noise

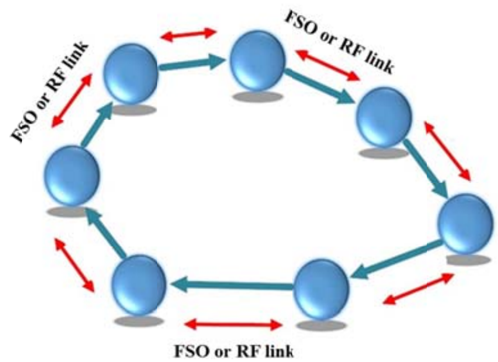

Fig. 2. An adaptive incremental network that can be implemented through RF or FSO links.

(AWGN) [12]. Also, the channel coefficients are considered to follow the Gamma-Gamma distribution [8] or the Log-normal distribution [9-11]. The Gamma-Gamma distribution is the best for modeling high turbulence levels. In this paper, we selected the Log-normal distribution which is the best for modeling Weak and Moderate turbulence levels and Gamma-Gamma distribution for modeling strong turbulence. Other references [11-17] also considered the FSO channel in detail. In reference [6] only 3 distributions namely the Negative exponential distribution, the Gamma-Gamma and Log-normal distributions were described for MATLAB software and the K-distribution can be derived from the Gamma-Gamma distribution by considering $\beta = 1$. Also, the negative exponential distribution can be derived from the Gamma-Gamma distribution by considering $\alpha \to \infty$ and $\beta = 1$ these information can be found in reference [12]. Using the information in these references, we modeled the FSO links and implemented the adaptive incremental network using these links.

The paper is organized as follows: In Section II, we present the system model and problem formulation. Also, the detail descriptions of the FSO channel models are given in Section II. The steady-state analysis of the ILMS algorithm with FSO links is given in section III. In Section IV, we present the simulation and theoretical results and compared them to support the proposed idea. Finally, in Section V we have our concluding remarks.

Notation: We used small boldface letters to represent vectors and capital boldface letters for matrices. The symbol $[.]^*$ denotes complex conjugate for scalars and Hermitian transposition for matrices. Also, the operator $\boldsymbol{E}[.]$ represents statistical expectation and the notation $\|.\|$ is used for representing the Euclidian norm of a vector.

II. Problem statement and link descriptions

Now, we consider an incremental network with N nodes. The node k at iteration i has access to the measurement $d_{k,i}$ and the regression input vector $\boldsymbol{u}_{k,i}$. The linear relation between these values is:

$$d_{k,i} = \boldsymbol{u}_{k,i}\boldsymbol{w}^o + v_{k,i} \tag{1}$$

where the $M \times 1$ unknown weight vector $\boldsymbol{w}^o = [w^o(1), w^o(2), \dots, w^o(M)]^T$ is the main goal in the estimation process of the network. This goal can be achieved by the following minimization:

$$arg \min_{\boldsymbol{w}} \left(\sum_{k=1}^{N} \boldsymbol{E} \left[\left| d_{k,i} - \boldsymbol{u}_{k,i} \boldsymbol{w} \right|^2 \right] \right) \tag{2}$$

In this case, the answer is:

$$\boldsymbol{w}^o = \left(\sum_{k=1}^{N} \boldsymbol{R}_{\boldsymbol{u},k} \right)^{-1} \left(\sum_{k=1}^{N} \boldsymbol{c}_{d\boldsymbol{u},k} \right) \tag{3}$$

where $\boldsymbol{R}_{\boldsymbol{u},k} = \boldsymbol{E}[\boldsymbol{u}_{k,i}^* \boldsymbol{u}_{k,i}]$ and $\boldsymbol{c}_{d\boldsymbol{u},k} = \boldsymbol{E}[d_{k,i} \boldsymbol{u}_{k,i}^*]$ are the regression input covariance matrix and the input- measurement cross-covariance vector respectively. Also, we consider the regression inputs and observation noise variables follow the Gaussian distribution and therefore their covariance matrices become $\boldsymbol{R}_{\boldsymbol{u},k} = \sigma_u^2 \boldsymbol{I}$ and $\boldsymbol{R}_{\boldsymbol{v},k} = \sigma_v^2 \boldsymbol{I}$ where the $\boldsymbol{I}$ represents the $M \times M$ unit matrix. As the exact values of $\boldsymbol{R}_{\boldsymbol{u},k}$ and $\boldsymbol{c}_{d\boldsymbol{u},k}$ are not available in most cases, the aim of the network is to converge to the $\boldsymbol{w}^o$ gradually using the distributed adaptive methods. In incremental strategy, each node k shares its local estimation of weight vector with its immediate neighbor $k+1$ and plays as the initial estimation for the next node. The incremental LMS (ILMS) algorithm is given as [8]:

For each time $i \geq 0$ repeat:

$$\begin{cases} \boldsymbol{\psi}_{0,i} \leftarrow \boldsymbol{w}_{N,i-1} \\ \boldsymbol{\psi}_{k,i} = \boldsymbol{\psi}_{k-1,i} + \mu_k \boldsymbol{u}_{k,i}^* \left(d_{k,i} - \boldsymbol{u}_{k,i} \boldsymbol{\psi}_{k-1,i} \right) \end{cases} \tag{4}$$

where μ_k is the step-size. In this strategy, $\boldsymbol{\psi}_{k,i}$ is the local estimation of unknown weight vector at iteration i on the node k. For each iteration and each node, the computational complexity of the ILMS algorithm is $2M+1$ multiplications and $2M$ additions for real-valued data and $8M+2$ multiplications and $8M$ additions for complex-valued data where M is the size of the optimum weight vector $\boldsymbol{w}^o$ which is 4 in this paper. For other algorithms and other network topologies, these values might be different [24].

A. Considering the FSO channel

Implementing wireless sensor networks using wireless optical communication technology has various benefits including the secure communication and using unregistered bandwidth. However, when we assume that the incremental network work through FSO channels as in Figure 3, the shared local estimation of the previous node is not exactly the same and is contaminated with channel noise and irradiance:

Therefore, the received local estimation by node k would be:

$$\boldsymbol{r}_{k,i} = I_{k,i} \boldsymbol{\psi}_{k-1,i} + \boldsymbol{q}_{k,i} \tag{5}$$

in this relation $I_{k,i}$ are the channel irradiance coefficients with mean $m_k = \boldsymbol{E}[I_{k,i}]$ and second order moment $s_k = \boldsymbol{E}[I_{k,i}^2]$ and $\boldsymbol{q}_{k,i}$ denotes the $M \times 1$ channel noise vector with the covariance matrix $\boldsymbol{Q}_k = \sigma_c^2 \boldsymbol{I}$. With this assumption, the updating relation of ILMS algorithm changes to:

$$\boldsymbol{\psi}_{k,i} = \boldsymbol{r}_{k,i} + \mu_k \boldsymbol{u}_{k,i}^* \left(d_{k,i} - \boldsymbol{u}_{k,i} \boldsymbol{r}_{k,i} \right) \tag{6}$$

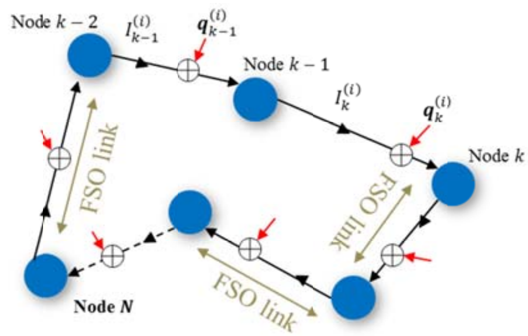

Fig. 3. The incremental adaptive network with FSO channels infected with channel noise and irradiance.

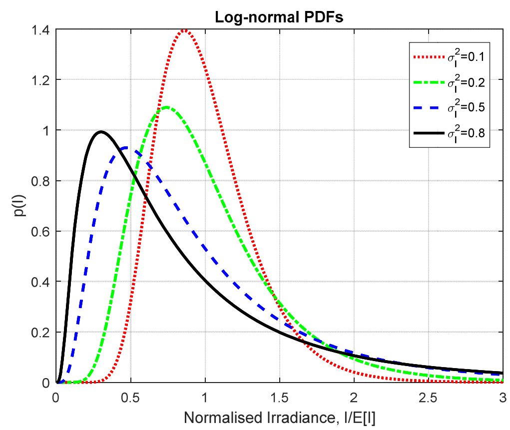

Fig. 4. The PDFs of Log-normal distribution for different values of the log irradiance variance.

and by replacing (6) in (4) we have:

$$\boldsymbol{\psi}_{k,i} = I_{k,i}\boldsymbol{\psi}_{k-1,i} + \boldsymbol{q}_{k,i} + \mu_k \boldsymbol{u}^* \left(d_{k,i} - \boldsymbol{u}_{k,i}\left(I_{k,i}\boldsymbol{\psi}_{k-1,i} + \boldsymbol{q}_{k,i}\right)\right) \tag{7}$$

Surely, the influence of these noise and channel coefficients will degrade channel performance which we will examine in this paper precisely. In Fig. 3, the channel irradiance coefficients $I_{k,i}$ are assumed to follow Log-normal and Gamma-Gamma distributions that we will explain more in detail:

B. The Log-normal channel model

One of the most common distributions in modeling the channel turbulence coefficients is the famous Log-normal distribution [5, 6]. This distribution has been suggested by performing various experiments and these experiments suggested important characteristics about modeling FSO channels with this distribution. The probability density function (PDF) of this distribution is given as [6]:

$$p(I) = \frac{1}{\sqrt{2\pi\sigma_l^2}}\frac{1}{I} exp\left\{-\frac{\left(ln\left({}^{I}/{}_{I_0}\right)-\boldsymbol{\mu}\right)^2}{2\sigma_l^2}\right\} \quad I \geq 0 \tag{8}$$

Table. I. The statistical values of the Log-normal channel.

For Log-normal model			
σ_l^2	μ	$\boldsymbol{E}[I] = m_k$	$\boldsymbol{E}[I^2] = s_k$
0.1	-0.005	1	1.01
0.2	-0.02	1	1.04
0.5	-0.125	1	1.284
0.8	-0.32	1	1.896

where $\sigma_l^2 = 1.23 C_n^2 k^{7/6} L_p^{11/6}$ is the log irradiance variance for a plane wave and the experiments showed that it usually takes the values of 0.1, 0.2, 0.5 and 0.8. For these values, the PDF of this distribution is shown in Fig. 4, [6]. Also, we have $\mu = -\frac{\sigma_l^2}{2}$.

In [1] it was expressed that the most important characteristics of the channel model that affects the network performance are the mean and second order moment. Therefore, for the presented σ_l^2 values we calculate these statistical characteristics and showed the results in Table. I.

The increase in the σ_l^2 value, makes the channel coefficients to fluctuate more and this causes the increase in turbulence level.

C. The Gamma-Gamma channel model

In this section, we introduce the Gamma-Gamma distribution that can model all the FSO channel turbulence levels from weak to strong. in the Gamma-Gamma distribution, the channel coefficients are generated from the multiplication of two Gamma variables [6]:

$$I = I_x I_y \tag{9}$$

where I_x and I_y follow the ordinary Gamma distribution and therefore we have:

$$p(I) = \frac{2(\alpha\beta)^{(\alpha+\beta)/2}}{\Gamma(\alpha)\Gamma(\beta)} I^{\left(\frac{\alpha+\beta}{2}\right)-1} K_{\alpha-\beta}\left(2\sqrt{\alpha\beta I}\right), \quad I > 0 \tag{10}$$

where $K_n(.)$ is the modified Bessel function of 2nd kind of order n, and $\Gamma(.)$ represents the Gamma function. The parameters α and β in this PDF is given by [8]:

$$\alpha = \left[exp\left(\frac{0.49\sigma_l^2}{\left(1+1.11\sigma_l^{12/5}\right)^{7/6}}\right) - 1\right]^{-1} \tag{11}$$

$$\beta = \left[exp\left(\frac{0.51\sigma_l^2}{\left(1+069\sigma_l^{12/5}\right)^{5/6}}\right) - 1\right]^{-1} \tag{12}$$

where $\sigma_l^2 = 1.23 C_n^2 k^{7/6} L^{11/6}$ is the log irradiance variance parameter, L is the link range, $k = \frac{2\pi}{\lambda}$, and $C_n^2 = 5.10^{-13}\ m^{-2/3}$. The values of α and β determine the level of channel turbulence. In Table. II, the specific values of α and β for weak, moderate and strong turbulences and their respective statistical values are given.

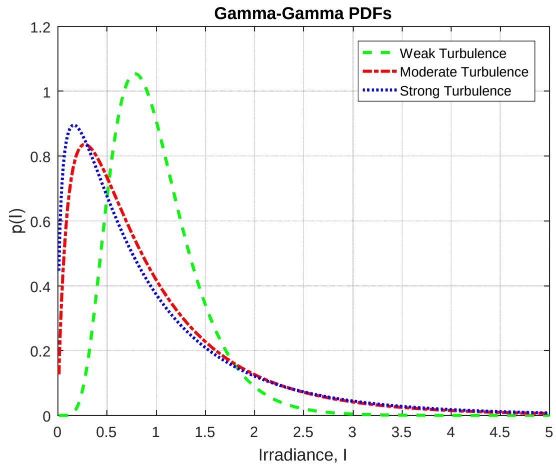

Fig. 5. The Gamma-Gamma PDFs for different turbulence levels of the FSO channel.

Table. II. The statistical values of the Gamma-Gamma channel.

Turbulence intensity	**Parameters**		**Statistical values**	
	α	β	$\boldsymbol{E}[I] = m_k$	$\boldsymbol{E}[I^2] = s_k$
Weak	11.6	10.1	1	1.13
Moderate	4.0	1.9	1	1.76
Strong	4.2	1.4	1	2.09

Using these values the PDFs of the Gamma-Gamma distributions for different turbulence levels are given in Fig. 5.

III. Mean square performance of ILMS algorithm

In this section, we analyze the mean stability and steady-state mean-square performance of the ILMS algorithm with the FSO link assumptions. Our analysis is based on the energy conservation relations of [6]. For this we define the following errors:

$$e_{k,i} = d_{k,i} - \boldsymbol{u}_{k,i}\boldsymbol{\psi}_{k-1,i}$$
$$\widetilde{\boldsymbol{\psi}}_{k,i} \triangleq \boldsymbol{w}^o - \boldsymbol{\psi}_{k,i} \tag{13}$$

Now, if we subtract $\boldsymbol{w}^o$ from both sides of equation (7) and replace $\widetilde{\boldsymbol{\psi}}_{k,i}$ where necessary then we have:

$$\widetilde{\boldsymbol{\psi}}_{k,i} = I_{k,i}\widetilde{\boldsymbol{\psi}}_{k-1,i} + \left(1 - I_{k,i}\right)\boldsymbol{w}^o - \mu_k I_{k,i}\boldsymbol{u}^*_{k,i}\boldsymbol{u}_{k,i}\widetilde{\boldsymbol{\psi}}_{k-1,i} - \mu_k \boldsymbol{u}^*_{k,i}\boldsymbol{v}_{k,i}$$
$$-\mu_k\left(1 - h_{k,i}\right)\boldsymbol{u}^*_{k,i}\boldsymbol{u}_{k,i}\boldsymbol{w}^o - \boldsymbol{q}_{k,i} + \mu_k\boldsymbol{u}^*_{k,i}\boldsymbol{u}_{k,i}\boldsymbol{q}_{k,i} \tag{14}$$

In [1] it was mentioned that the convergence condition for choosing the step-size parameter of the incremental LMS algorithm in FSO links is:

$$max\left\{0, \frac{m_k - 1}{m_k\lambda_{min}(\boldsymbol{R}_{u,k})}\right\} < \mu_k < \frac{m_k + 1}{m_k\lambda_{max}(\boldsymbol{R}_{u,k})} \tag{15}$$

This condition shows that the value of step-size directly depends on the coefficient means (m_k) of FSO channel and therefore depends on the channel model that we assumed. To prove this convergence condition we must use some definitions [1]. Using (13) we have:

$$\boldsymbol{E}[\widetilde{\boldsymbol{\psi}}_{k,i}] = m_k \mathbf{J}_k \boldsymbol{E}[\widetilde{\boldsymbol{\psi}}_{k-1,i}] + (1-m_k)\mathbf{J}_k \boldsymbol{w}^o \quad (16)$$

where:

$$\mathbf{J}_k \triangleq \boldsymbol{I} - \mu_k \boldsymbol{R}_{u,k} \quad (17)$$

By considering iteration in (16) we get:

$$\boldsymbol{E}[\widetilde{\boldsymbol{\psi}}_{k,i}] = \left(\prod_{n=1}^{N} m_n \mathbf{J}_n\right)\boldsymbol{E}[\widetilde{\boldsymbol{\psi}}_{k,i-1}] + \sum_{n=1}^{N}\left((1-m_n)\mathbf{J}_n \prod_{l=n+1}^{N} m_l \mathbf{J}_l\right)\boldsymbol{w}^o \quad (18)$$

For analyzing the convergence condition we define the $\boldsymbol{\mathcal{M}}$ matrix:

$$\boldsymbol{\mathcal{M}} \triangleq \prod_{n=1}^{N} m_n \mathbf{J}_n \quad (19)$$

In order to converge, all Eigen values of this matrix must be inside the unit circle:

$$\rho(\boldsymbol{\mathcal{M}}) < 1 \quad (20)$$

In other words we must have [1]:

$$\rho(\boldsymbol{\mathcal{M}}) \le \|\boldsymbol{\mathcal{M}}\| \le \|m_1\mathbf{J}_1\|\|m_2\mathbf{J}_2\| \ldots \|m_N\mathbf{J}_N\| = \rho(m_1\mathbf{J}_1)\rho(m_2\mathbf{J}_2)\ldots\rho(m_N\mathbf{J}_N)$$

In order to satisfy the constraint of (20) it is sufficient to have $\rho(m_1\mathbf{J}_k) \le 1$this entails:

$$|m_k(1-\mu_k\lambda)| < 1 \quad (21)$$

Therefore, the limits for step-size are pointed out using:

$$max\left\{0, \frac{m_k - 1}{m_k \lambda_{min}(\boldsymbol{R}_{u,k})}\right\} < \mu_k < \frac{m_k + 1}{m_k \lambda_{max}(\boldsymbol{R}_{u,k})}$$

and therefore the convergence condition is proven to be the same as in [1]. Also, by considering this condition we have:

$$\lim_{i\to\infty} \boldsymbol{E}[\widetilde{\boldsymbol{\psi}}_{k,i}] = (I - \boldsymbol{\mathcal{M}})^{-1} \sum_{n=1}^{N}\left((1-m_n)\mathbf{J}_n \prod_{l=n+1}^{N} m_l\, \mathbf{J}_l\right)\boldsymbol{w}^o$$

(22)

Now, in order to analyze the mean square performance of the ILMS algorithm we define the following performance criteria [8]:

$$MSD_k \triangleq \lim_{i\to\infty} \boldsymbol{E}\left[\left\|\widetilde{\boldsymbol{\psi}}_{k-1,i}\right\|_{\boldsymbol{I}}^2\right]$$

(23)

$$EMSE_k \triangleq \lim_{i\to\infty} \boldsymbol{E}\left[\left\|\widetilde{\boldsymbol{\psi}}_{k-1,i}\right\|_{\boldsymbol{R}_{u,k}}^2\right]$$

(24)

$$MSE_k \triangleq \lim_{i\to\infty} \boldsymbol{E}\left[\left|e_{k,i}\right|^2\right] = EMSE_k + \sigma_{v,k}^2 \quad (25)$$

We define:

$$\boldsymbol{C}_{k,i} \triangleq m_k \mathbf{J}_k \boldsymbol{C}_{k-1,i} + (1-m_k)\mathbf{J}_k \quad (26)$$

In this relation $\boldsymbol{C}_{0,i} = \boldsymbol{C}_{N,i-1}$ also $\boldsymbol{C}_{0,1} = \boldsymbol{I}$. We can write:

$$\boldsymbol{E}[\widetilde{\boldsymbol{\psi}}_{k,i}] = \boldsymbol{C}_{k,i}\boldsymbol{w}^o \quad (27)$$

If we apply the weighted norm operation in both sides of equation (14) and take expectation of them we get:

$$\boldsymbol{E}\left[\left\|\widetilde{\boldsymbol{\psi}}_{k,i}\right\|_{\boldsymbol{\Sigma}_k}^2\right] = \boldsymbol{E}\left[\left\|\widetilde{\boldsymbol{\psi}}_{k-1,i}\right\|_{\boldsymbol{\Sigma}'_k}^2\right] + \mu_k^2\sigma_{v,k}^2\boldsymbol{E}\left[\left\|\boldsymbol{u}_{k,i}\right\|_{\boldsymbol{\Sigma}_k}^2\right] + \boldsymbol{E}\left[\left\|\boldsymbol{q}_{k,i}\right\|_{\mathbf{G}_k}^2\right] + \|\boldsymbol{w}^o\|_{(\boldsymbol{T}_k+\boldsymbol{H}_{k,i})}^2 \quad (28)$$

In this recursive relation we have:

$$\boldsymbol{G}_k = \boldsymbol{\Sigma}_k - \mu_k\boldsymbol{E}\left[\boldsymbol{\Sigma}_k\boldsymbol{u}_{k,i}^*\boldsymbol{u}_{k,i} + \boldsymbol{u}_{k,i}^*\boldsymbol{u}_{k,i}\boldsymbol{\Sigma}_k\right] + \mu_k^2\boldsymbol{E}\left[\left\|\boldsymbol{u}_{k,i}\right\|_{\boldsymbol{\Sigma}_k}^2\boldsymbol{u}_{k,i}^*\boldsymbol{u}_{k,i}\right] \quad (29)$$

where we consider the following relations:

$$\boldsymbol{\Sigma}'_k = s_k\boldsymbol{G}_k \quad (30)$$

$$\boldsymbol{T}_k = (1 - 2m_k + s_k)\boldsymbol{G}_k \quad (31)$$

$$\boldsymbol{H}_{k,i} = (m_k - s_k)\left(\boldsymbol{C}_{k-1,i}\boldsymbol{G}_k + \boldsymbol{G}_k\boldsymbol{C}_{k-1,i}\right) \quad (32)$$

$$\boldsymbol{R}_{u,k} = \boldsymbol{U}_k\boldsymbol{\Lambda}_k\boldsymbol{U}_k^* \quad (33)$$

also, we define [1]:

$$\begin{aligned}
&\overline{\boldsymbol{\psi}}_{k,i} = \boldsymbol{U}_k^*\widetilde{\boldsymbol{\psi}}_{k,i},\ \overline{\boldsymbol{\Sigma}}_k = \boldsymbol{U}_k^*\boldsymbol{\Sigma}_k\boldsymbol{U}_k,\\
&\overline{\boldsymbol{\Sigma}}'_k = \boldsymbol{U}_k^*\boldsymbol{\Sigma}'_k\boldsymbol{U}_k,\ \overline{\mathbf{u}}_{k,i} = \mathbf{u}_{k,i}\boldsymbol{U}_k,\\
&\overline{\mathbf{T}}_k = \boldsymbol{U}_k^*\mathbf{T}_k\boldsymbol{U}_k,\ \overline{\mathbf{H}}_{k,i} = \boldsymbol{U}_k^*\mathbf{H}_{k,i}\boldsymbol{U}_k,\\
&\overline{\boldsymbol{w}}^o = \boldsymbol{U}_k^*\boldsymbol{w}^o, \qquad \overline{\mathbf{C}}_{k-1,i} = \boldsymbol{U}_k^*\mathbf{C}_{k-1,i}\boldsymbol{U}_k,\\
&\overline{\mathbf{Q}}_k = \boldsymbol{U}_k^*\mathbf{Q}_k\boldsymbol{U}_k, \qquad \boldsymbol{W} = \overline{\boldsymbol{w}}^o\overline{\boldsymbol{w}}^{o*} = \boldsymbol{w}^o\boldsymbol{w}^{o*}
\end{aligned}$$

By considering these definitions, the equation (25) can be written as:

$$\boldsymbol{E}\left[\left\|\overline{\boldsymbol{\psi}}_{k,i}\right\|_{\overline{\boldsymbol{\Sigma}}_k}^2\right] = \boldsymbol{E}\left[\left\|\overline{\boldsymbol{\psi}}_{k-1,i}\right\|_{\overline{\boldsymbol{\Sigma}}'_k}^2\right] + \mu_k^2\sigma_{v,k}^2\boldsymbol{E}\left[\left\|\overline{\boldsymbol{u}}_{k,i}\right\|_{\overline{\boldsymbol{\Sigma}}_k}^2\right] + \boldsymbol{E}\left[\left\|\overline{\boldsymbol{q}}_{k,i}\right\|_{\overline{\mathbf{G}}_k}^2\right] + \|\overline{\boldsymbol{w}}^o\|_{(\overline{\boldsymbol{T}}_k+\overline{\boldsymbol{H}}_{k,i})}^2 \quad (34)$$

where:

$$\overline{\boldsymbol{G}}_k = \overline{\boldsymbol{\Sigma}}_k - \mu_k\boldsymbol{E}\left[\overline{\boldsymbol{\Sigma}}_k\overline{\boldsymbol{u}}_{k,i}^*\overline{\boldsymbol{u}}_{k,i} + \overline{\boldsymbol{u}}_{k,i}^*\overline{\boldsymbol{u}}_{k,i}\overline{\boldsymbol{\Sigma}}_k\right] + \mu_k^2\boldsymbol{E}\left[\left\|\overline{\boldsymbol{u}}_{k,i}\right\|_{\overline{\boldsymbol{\Sigma}}_k}^2\overline{\boldsymbol{u}}_{k,i}^*\overline{\boldsymbol{u}}_{k,i}\right] = \overline{\boldsymbol{\Sigma}}_k - \mu_k(\overline{\boldsymbol{\Sigma}}_k\boldsymbol{\Lambda}_k + \boldsymbol{\Lambda}_k\overline{\boldsymbol{\Sigma}}_k) + \mu_k^2(\boldsymbol{\Lambda}_k tr[\overline{\boldsymbol{\Sigma}}_k\boldsymbol{\Lambda}_k] + \boldsymbol{\Lambda}_k\overline{\boldsymbol{\Sigma}}_k\boldsymbol{\Lambda}_k) \quad (35)$$

and we have:

$$\overline{\boldsymbol{\Sigma}}'_k = s_k\overline{\boldsymbol{G}}_k \quad (36)$$

$$\overline{\boldsymbol{T}}_k = (1 - 2m_k + s_k)\overline{\boldsymbol{G}}_k$$

$$\overline{\boldsymbol{H}}_{k,i} = (m_k - s_k)\left(\overline{\boldsymbol{C}}_{k-1,i}\overline{\boldsymbol{G}}_k + \overline{\boldsymbol{G}}_k\overline{\boldsymbol{C}}_{k-1,i}\right) \quad (37)$$

We can write:

$$\boldsymbol{E}\left[\left\|\overline{\boldsymbol{\psi}}_{k,i}\right\|_{\overline{\boldsymbol{\Sigma}}_k}^2\right] = \boldsymbol{E}\left[\left\|\overline{\boldsymbol{\psi}}_{k-1,i}\right\|_{\overline{\boldsymbol{\Sigma}}'_k}^2\right] + \mu_k^2\sigma_{v,k}^2 tr[\boldsymbol{\Lambda}_k\overline{\boldsymbol{\Sigma}}_k] + tr[\overline{\mathbf{Q}}_k\overline{\mathbf{G}}_k] + tr[\boldsymbol{W}\overline{\mathbf{T}}_k] + tr\left[\boldsymbol{W}\overline{\mathbf{H}}_{k,i}\right] \quad (38)$$

By the following definitions:

$$\overline{\boldsymbol{\sigma}}_k \triangleq diag[\overline{\boldsymbol{\Sigma}}_k], \qquad \overline{\boldsymbol{\sigma}}'_k \triangleq diag[\overline{\boldsymbol{\Sigma}}'_k], \qquad \boldsymbol{\lambda}_k \triangleq diag[\boldsymbol{\Lambda}_k] \quad (39)$$

and

$$\overline{\boldsymbol{F}}_k \triangleq \boldsymbol{I} - \mu_k 2\boldsymbol{\Lambda}_k + \mu_k^2\boldsymbol{\Lambda}_k^2 + \boldsymbol{\lambda}_k\boldsymbol{\lambda}_k^T \quad (40)$$

we have:

$$\boldsymbol{E}\left[\left\|\overline{\boldsymbol{\psi}}_{k,i}\right\|_{\overline{\boldsymbol{\sigma}}_k}^2\right] = \boldsymbol{E}\left[\left\|\overline{\boldsymbol{\psi}}_{k-1,i}\right\|_{\overline{\boldsymbol{\sigma}}'_k}^2\right] + g_{k,i}\overline{\boldsymbol{\sigma}}_{\boldsymbol{k}} \quad (41)$$

where:

$$\boldsymbol{g}_{k,i} = \mu_k^2\sigma_{v,k}^2\boldsymbol{\lambda}_k^T + (diag[\overline{\boldsymbol{Q}}_k])^T\overline{\boldsymbol{F}}_k + (1-2m_k+s_k)(diag[\boldsymbol{W}])^T\overline{\boldsymbol{F}}_k$$
$$+2(m_k - s_k)(diag[\boldsymbol{W}])^T\overline{\boldsymbol{C}}_{k-1,i}\,\overline{\boldsymbol{F}}_k \tag{42}$$

and also we have:

$$\overline{\boldsymbol{\sigma}}_k' = s_k\overline{\boldsymbol{F}}_k\overline{\boldsymbol{\sigma}}_k \tag{43}$$

Now, if we choose a sufficiently small step size so that:

$$s_k\rho(\overline{\boldsymbol{F}}_k) < 1 \tag{44}$$

we get to the following relation for $i > 0$:

$$\boldsymbol{E}\left[\left\|\overline{\boldsymbol{\psi}}_{k,i}\right\|_{\overline{\boldsymbol{\sigma}}_{\boldsymbol{k}}}^2\right] = \boldsymbol{E}\left[\left\|\overline{\boldsymbol{\psi}}_{k,i-1}\right\|_{\boldsymbol{\mathcal{F}}_{k+1,1}\overline{\boldsymbol{\sigma}}_k}^2\right] + a_{k+1,i}\overline{\boldsymbol{\sigma}}_k \tag{45}$$

where we used the following definitions:

$$\boldsymbol{\mathcal{F}}_{k+1,1} \triangleq (s_{k+l-1}\overline{\boldsymbol{F}}_{k+l-1})(s_{k+l}\overline{\boldsymbol{F}}_{k+l}) \ldots (s_N\overline{\boldsymbol{F}}_N)(s_1\overline{\boldsymbol{F}}_1) \ldots (s_{k-1}\overline{\boldsymbol{F}}_{k-1}) \tag{46}$$

$$\boldsymbol{a}_{k,i} \triangleq \boldsymbol{g}_{k,i}\boldsymbol{F}_{k,2} + \boldsymbol{g}_{k+1,i}\boldsymbol{F}_{k,3} + \cdots \boldsymbol{g}_{k-2,i}\boldsymbol{F}_{k,N} + \boldsymbol{g}_{k-1,i} \tag{47}$$

Also, as for small step sizes as the iteration number goes to infinity ($i \to \infty$) we have:

$$\boldsymbol{E}\left[\left\|\overline{\boldsymbol{\psi}}_{k,\infty}\right\|_{\overline{\boldsymbol{\sigma}}_{\boldsymbol{k}}}^2\right] = \boldsymbol{E}\left[\left\|\overline{\boldsymbol{\psi}}_{k-1,\infty}\right\|_{\overline{\boldsymbol{\sigma}}_{\boldsymbol{k}}'}^2\right] + \boldsymbol{g}_{k,\infty}\overline{\boldsymbol{\sigma}}_{\boldsymbol{k}} \tag{48}$$

Then, the steady-state metrics in FSO environment become:

$$MSD_k = \boldsymbol{a}_{k,\infty}\left(\boldsymbol{I} - \boldsymbol{\mathcal{F}}_{k,1}\right)^{-1} diag[\boldsymbol{I}] \tag{49}$$

$$EMSE_k \triangleq \boldsymbol{a}_{k,\infty}\left(\boldsymbol{I} - \boldsymbol{\mathcal{F}}_{k,1}\right)^{-1}\boldsymbol{\lambda}_k \tag{50}$$

$$MSE_k \triangleq EMSE_k + \sigma_{v,k}^2 \tag{51}$$

Then, according to (47) we must determine $\boldsymbol{g}_{k,\infty}$ using (41). Therefore with the help of (25) we have:

$$\overline{\boldsymbol{C}}_{k-1,\infty} = \boldsymbol{U}_k^*\left((\boldsymbol{I} - \boldsymbol{\mathcal{M}})^{-1} \times \textstyle\sum_{n=1}^N\left((1-m_n)\mathbf{J}_n\prod_{l=n+1}^N m_l\mathbf{J}_l\right)\right)\boldsymbol{U}_k \tag{52}$$

In [1] it has been assumed that $m_k = 1$ for all nodes and this term was canceled out from the later calculations. In this paper however, we consider the following assumptions:

1) $m_k = 1, \quad \boldsymbol{R}_{u,k} = \sigma_{u,k}^2\boldsymbol{I}, \qquad \boldsymbol{Q}_k = \sigma_{c,k}^2\boldsymbol{I}$
2) $\overline{\boldsymbol{F}}_k \approx \left(1 - 2\mu\sigma_{u,k}^2\right)\boldsymbol{I}$

Because $\overline{\boldsymbol{F}}_k$ is diagonal, we have $\boldsymbol{\mathcal{F}}_{k,l} \approx \overline{\boldsymbol{F}}_1\overline{\boldsymbol{F}}_2 \ldots \overline{\boldsymbol{F}}_N$ and we can write:

$$\boldsymbol{\mathcal{F}}_{k,l} \approx s_p\left(1 - 2\mu\sigma_{u,k}^2\right)^N\boldsymbol{I} \tag{53}$$

If we define $s_p \triangleq \prod_{k=1}^N s_k$ we can write:

$$\boldsymbol{I} - \boldsymbol{\mathcal{F}}_{k,l} \approx \left(1 - s_p\left(1 - 2\mu\sigma_{u,k}^2\right)^N\right)\boldsymbol{I} \tag{54}$$

Now, we can approximate $\boldsymbol{g}_{k,\infty}$ and $a_{k,\infty}$:

$$\boldsymbol{g}_{k,\infty} \approx \left(\mu_k^2\sigma_{v,k}^2\sigma_{u,k}^2\right)(diag[\boldsymbol{I}])^T + \left(\sigma_{c,k}^2\left(1-2\mu\sigma_{u,k}^2\right)\right)(diag[\boldsymbol{I}])^T$$
$$+ s_p(1-2m_k+s_k)\left(1-2\mu\sigma_{u,k}^2\right)(diag[\boldsymbol{W}])^T + 2(m_k-s_k)(diag[\boldsymbol{W}])^T\overline{\boldsymbol{C}}_{k-1,\infty}\,\overline{\boldsymbol{F}}_k$$
$$\approx \left(\mu^2\sigma_{v,k}^2\sigma_{u,k}^2 + \sigma_{c,k}^2\left(1-2\mu\sigma_{u,k}^2\right)\right)(diag[\boldsymbol{I}])^T$$
$$+ s_p(1-2m_k+s_k)\left(1-2\mu\sigma_{u,k}^2\right)(diag[\boldsymbol{W}])^T + 2(m_k-s_k)(diag[\boldsymbol{W}])^T\overline{\boldsymbol{C}}_{k-1,\infty}\,\overline{\boldsymbol{F}}_k$$
$$a_{k,\infty} = s_p\left(1-2\mu\sigma_{u,k}^2\right)^N\left(\textstyle\sum_{n=1}^N \boldsymbol{g}_{n,\infty} - \boldsymbol{g}_{k-1,\infty}\right) + \boldsymbol{g}_{k-1,\infty} \approx \left(s_p\left(1-2\mu\sigma_{u,k}^2\right)^N\right)\textstyle\sum_{n=1}^N \boldsymbol{g}_{n,\infty} +$$
$$\left(s_p\left(1-2\mu\sigma_{u,k}^2\right)^N\right)\boldsymbol{g}_{k-1,\infty} \tag{55}$$

Finally, we can derive the following relations for the steady-state behavior of ILMS algorithm under FSO conditions:

$$MSD_k \approx \left(\frac{1}{1-s_p(1-2\mu\lambda)^N} - 1\right)\sum_{n=1}^N f_n + f_{k-1} \tag{56}$$

where unlike [1] we incorporated $\overline{\boldsymbol{C}}_{k-1,\infty}$ in definition of f_k:

$$f_k = \left(\mu^2\sigma_{v,k}^2\sigma_{u,k}^2 + \sigma_{c,k}^2\left(1-2\mu\sigma_{u,k}^2\right)\right)M + s_p(1-2m_k+s_k)\left(1-2\mu\sigma_{u,k}^2\right)\|\boldsymbol{w}^o\|^2$$
$$+ s_p(m_k-s_k)\left(1-2\mu\sigma_{u,k}^2\right)\overline{\boldsymbol{C}}_{k-1,\infty}\|\boldsymbol{w}^o\|^2 \tag{57}$$

$$EMSE_k \approx \sigma_{u,k}^2\left(\frac{1}{1-s_p\left(1-2\mu\sigma_{u,k}^2\right)^N} - 1\right)\sum_{n=1}^N f_n + \sigma_{u,k}^2 f_{k-1} \tag{58}$$

in these equations, we can see the effect of m_k and s_k on the performance of the adaptive network. With the help of the entries in Table. 1 and Table II, we can see that these variables are dependent on the parameters of the Link. This criterion represents the dependence of network performance on the assumed FSO channel model. It means that if we change the parameters of the FSO link, we can directly observe the changes in estimation error performance and that is our contribution to this paper.

IV. Simulation results

As it was mentioned earlier, our intention in this paper is to investigate the performance of adaptive incremental networks implemented with the FSO technology both theoretically and with simulations. Now, it is the time to give the simulation results for various FSO channel conditions. We divide our results for the Log-normal and Gamma-Gamma channel models. For both of these models, the theoretical results are presented and compared with the simulation results. To perform our simulations we designed a network like Fig. 2 with 20 nodes. This network consists of nodes that can each performs local estimations with LMS algorithm and then share their information with the neighboring nodes via FSO links. The aim of this network in the estimation application is to converge to the $\boldsymbol{w}^o$ vector with the size of $M = 4$ and therefore we have $\boldsymbol{w}^o = \frac{1}{\sqrt{4}}[1\ 1\ 1\ 1]$. The convergence and the performance of the network depends on the Eigen values of the input covariance matrix $\boldsymbol{R}_{\boldsymbol{u},k}$. For all the nodes the step-size value μ is 0.02 because for all the simulations we considered $\lambda_{max} = 5$ and using the relation (15) we must choose the step-size value as $0 < \mu < 0.4$ for the convergence.

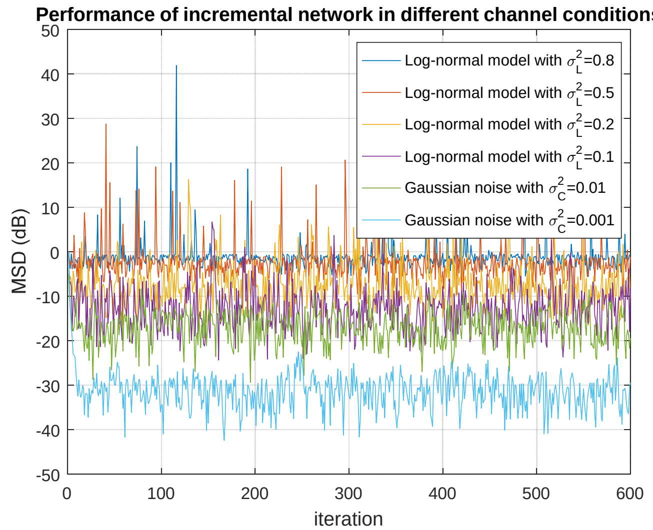

Fig. 6. The steady-state mean square deviation of incremental network in FSO channels.

The input data and the noise variables (both measurement noise and the channel noise) are produced with the Gaussian distribution. The measurement noise is the noise that contaminates the sensor measurement task and is shown in the paper with $v_{k,i}$, however, the link noise or channel noise contaminates the local estimations that are communicated between the nodes and is shown in the paper with $q_{k,i}$. Also, the Eigen spread of the covariance matrix of the input variables ($\boldsymbol{R}_{\boldsymbol{u},k}$) is considered to be between 1 and 5. As we mentioned the FSO channel among nodes is considered to be modeled with Log-normal distribution or with Gaussian noise.

For the theoretical results to match with the simulation ones the iteration number must be large enough. We are working with the adaptive algorithms, therefore after they are converged, the number of iterations is not important and the results will be the same for all the remaining iterations. The needed number of iterations for our network to converge is less than 100 (it depends on the number of the nodes, step-size value and the used algorithm) and after that, the mean square error results remain unchanged.

For our first simulation test, the MSD and EMSE of the incremental network are evaluated in different FSO channel conditions. In Fig. 5, it is presented that the MSD of the network in higher (moderate) turbulence conditions becomes unacceptable but for lower σ_l^2 values the network can converge to the desired vector suitably. Also, for the times that the channel turbulence does not exist and only the channel noise is present, the convergence error becomes very low according to the variance of channel noise (σ_c^2).

In the estimation task, it is important for us to know exactly how much we get close to the desired weight vector. Therefore these diagrams show the error amount (the difference between the estimated and desired weight vector) in different link conditions. In various papers, these diagrams have been given for numerous channel types and here, for the first time, we presented them for FSO links.

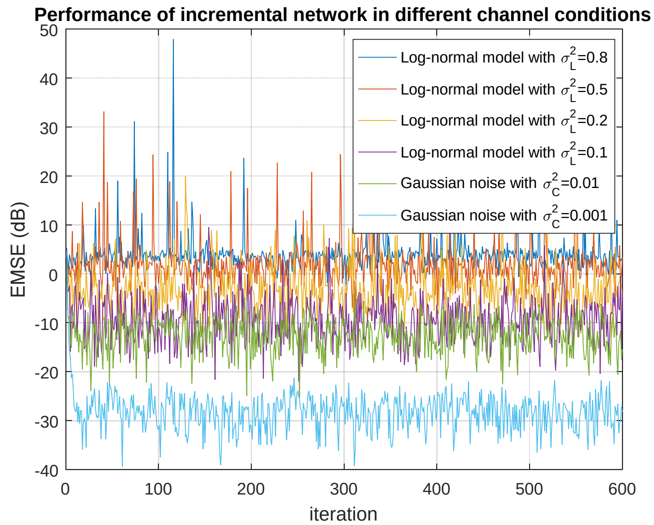

Fig. 7. The steady-state excess mean square error of incremental network in FSO channels.

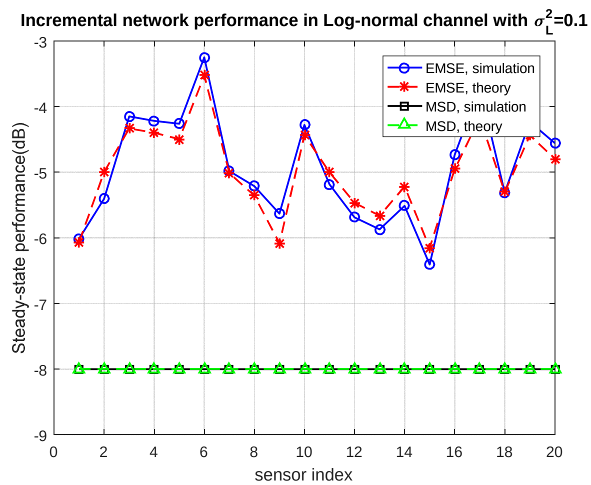

Fig. 8. The theoretical and simulated MSD and EMSE results of incremental network in Log-normal channel with $\sigma_l^2 = 0.1$.

The same remarks can be made for the EMSE of the incremental network in FSO channels in Fig. 7. For the second simulation, we assumed the incremental network with FSO Log-normal channel and $\sigma_l^2 = 0.1$. Both the resulted MSD and EMSE of simulations are compared with the theoretical error values that are acquired using relations (56) and (58). The results are shown in Fig. 8 and 9. It can be seen that there is a reasonable match between the theoretical and simulation outcomes.

For the third simulation again the FSO channel is considered to be Log-normal but this time with $\sigma_l^2 = 0.2$. Both the theoretical and simulation results were acquired for this test and the results are presented in Fig. 9. As we expected the results of this simulations are degraded in comparison with the previous simulation due to the increase of σ_l^2 value which is accordingly related to the worsening of the environmental conditions.

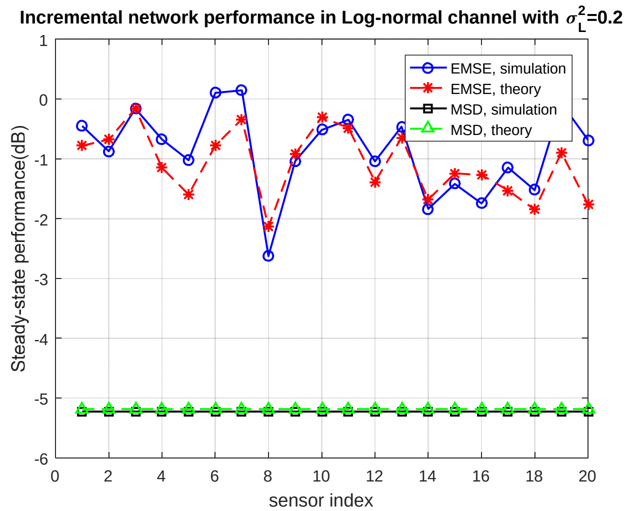

Fig. 9. The theoretical and simulated MSD and EMSE results of incremental network in Log-normal channel with $\sigma_l^2 = 0.2$.

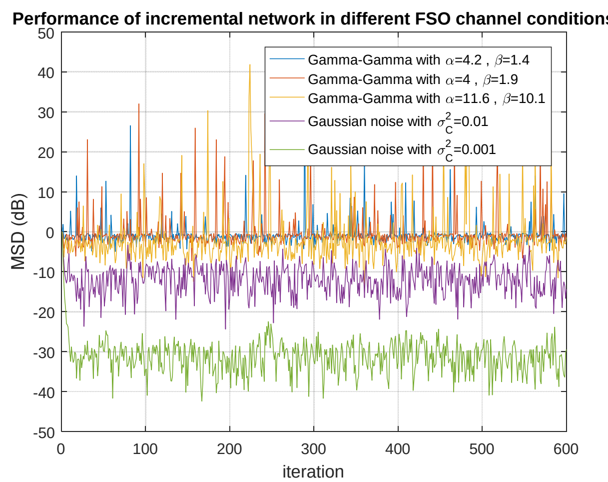

Fig. 10. Gamma_Gamma simulation results MSD

The FSO link model parameters for the Gamma-Gamma distribution are given in the simulation plots. Also, we performed simulations for the cases that the channel is not turbulent and only is contaminated with optical noise and the results are depicted according to the channel noise variance σ_c^2. We can see the outcome in MSD sense in Fig. 10. This performance analysis shows how close we can converge to the $\boldsymbol{w}^o$ vector by the incremental adaptive network when working through Gamma-Gamma FSO channels.

The other error criteria that we can examine the network performance with, is the EMSE. The performance of the incremental network in FSO channels in EMSE sense is given in Fig. 11. It is important to notice that for the times when the FSO channel is contaminated with Turbulence, the difference between the MSD and EMSE values become clearer and we can see that the EMSE values are a bit higher than the MSD values. For the noisy links, this difference is not noticeable.

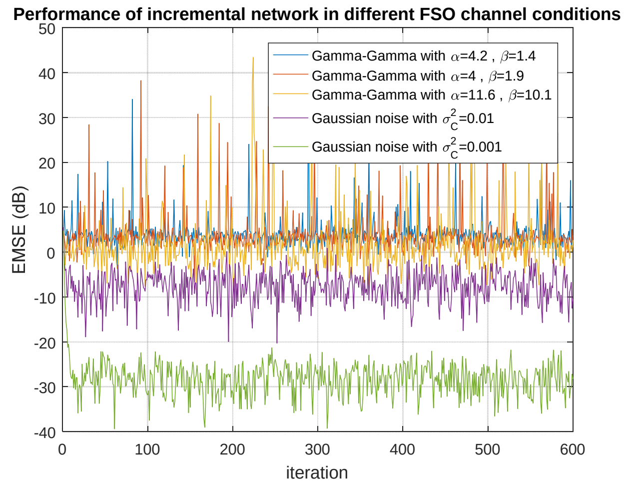

Fig. 11. Gamma_Gamma simulation results EMSE

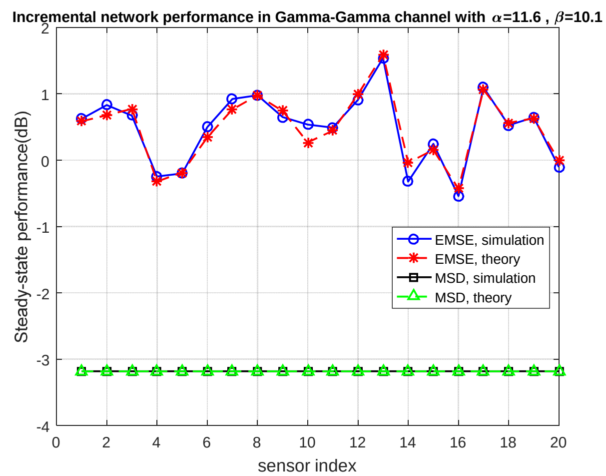

Fig. 12. Weak Gamma_Gamma Theoretical results

To compare the simulation results with the theoretical findings of relations (56) and (58) we performed 2 separate simulations and presented the results in both MSD and EMSE senses. The first simulation was conveyed for the Gamma-Gamma modeled FSO channel with weak turbulence regime and the results are depicted in Fig. 12.

As we can see there is a reasonable match between the theoretical and simulation results in Fig. 12 and this shows the credibility of our theoretical findings. The second comparison between the simulation and theoretical results was made for the Gamma-Gamma modeled FSO channel with the moderate turbulence level. The results are shown in Fig. 13.

In Fig. 13 also, there is a nearly perfect match between the simulated and theoretical results showing the exact anticipated error values for the incremental adaptive network that is implemented with the FSO communication technology.

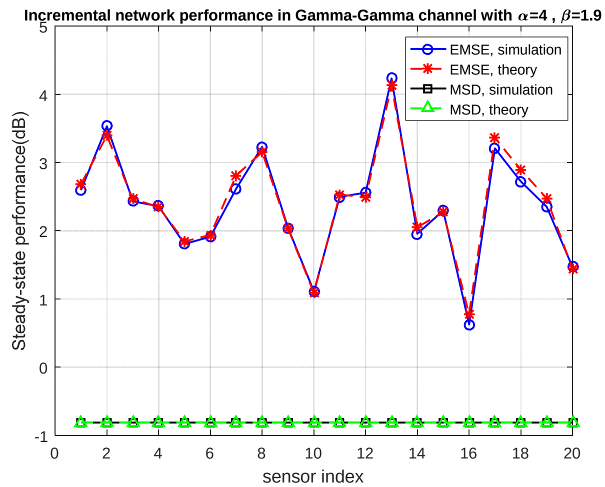

Fig. 13. Moderate Gamma_Gamma Theoretical results

IV. Conclusion

Adaptive networks can be used in different channel conditions for various applications. The important thing is how well they work in these conditions. In order to investigate this, we must perform both theoretical and simulation analysis depending on the exact values of link models. In this paper, we considered FSO channels that were impaired with Gaussian noisy and turbulence modeled with Log-normal and Gamma-Gamma distributions. Both the theoretical and simulation results showed the degradations that the adaptive incremental network face when using FSO links. We conclude that the when the turbulence level is low, the incremental network can perform its estimation reasonably but for the times that the links contaminated with high-level turbulence (as a result of variations in the refractive index of the atmosphere) some countermeasures like the channel estimation must be taken into the consideration for the performance improvement. In future works, we will analyze the performance of adaptive networks in other FSO channel models. Also, in future works, we will consider the time-varying channel estimation for FSO links with adaptive networks which will be a solution for the non-stationary channel condition.

References

[1] A. Khalili, A. Rastegarnia, and S. Sanei, “Performance analysis of incremental LMS over flat fading channels,” IEEE Trans. on control of network systems, vol. 4, no. 3, pp. 489 - 498, Sept. 2017.

[2] C. G. Lopes and A. H. Sayed, “Incremental adaptive strategies over distributed networks,” IEEE Trans. on signal processing, vol. 55, no. 8, pp. 4064- 4077, August 2007.

[3] A. H. Sayed and F. Cattivelli, “Distributed adaptive learning mechanisms,” in Handb. Array Process. Sens. Networks, S. Haykin and K. J. Ray Liu, Eds. Wiley, pp. 693-722, 2009.

[4] A. Rastegarnia, M. A. Tinati, and A. Khalili, “Steady-state analysis of incremental LMS adaptive networks with noisy links,” IEEE Trans. on Signal Process, vol. 59, no. 5, pp. 2416-2421, May 2011.

[5] A. Aminfar, Ch. Ghobadi, and M. Chehel Amirani, “Diffusion adaptation through free space optical (FSO) wireless communication channels,” IEEE 4th International Conference on Knowledge-Based Engineering and Innovation (KBEI-2017), Tehran, Iran, Dec. 22, 2017.

[6] Z. Ghassemlooy, W. Popoola, and S. Rajbhandari, “Optical wireless communications system and channel modeling with MATLAB,” CRC Press, NY, 2013.

[7] S. Rajbhandari, Z. Ghassemlooy, P. Haigh, T. Kanesan, and X. Tang, “Experimental error performance of modulation schemes under a controlled laboratory turbulence FSO channel,” Journal of Lightwave Technology, vol. 33, no. 1, pp. 244-250, Jan. 2015.

[8] P. V. Trinh et al., “BER analysis of all-optical AF dual-hop FSO systems over Gamma-Gamma channels,” Proc. of IEEE 4th International Conference on Photonics, pp. 175-177, Oct. 2013.

[9] X. Zhu and J. M. Kahn, “Performance bounds for coded free-space optical communications through atmospheric turbulence channels,” IEEE Trans. Commun., vol. 51, no. 8, pp. 1233-1239, Aug. 2003.

[10] M. T. Dabiri and M. Sajad Sadough, “Performance analysis of all-optical amplify and forward relaying over Log-Normal FSO channels,” J. Opt. Commu. NETW., vol. 10, no. 2, pp. 79-89, Feb. 2018.

[11] T. V. Pham, T. C. Thang, and A. T. Pham, “Performance Analysis of Multihop FSO Systems Using APD Receivers over Log-Normal Channels,” IEEE/CIC international conference on communications in China, pp. 165-170, Aug. 2013.

[12] M. Uysal, C. Capsoni, Z. Ghassemlooy, A.C. Boucouvalas, and E.G. Udvary (Eds.), Optical Wireless Communications - An Emerging Technology, Springer publications, page 237, 2016.

[13] M.D. Higgins, R.J. Green, and M.S. Leeson, “Optical wireless for intravehicle communications: A channel viability analysis,” IEEE Trans. Veh. Technol., vol. 61, no. 1, pp. 123-129, Jan. 2012.

[14] L. Yang, X. Gao, and M.-S. Alouini, “Performance analysis of relay-assisted all-optical FSO networks over strong atmospheric turbulence channels with pointing errors,” IEEE/OSA J. Lightw. Tech., vol. 32, no. 23, pp. 401-4018, Dec. 2014.

[15] J.-Y. Wang, J.-B. Wan, M. Chen, and X. Song, “Performance analysis for free-space optical communications using parallel all-optical relays over composite channels,” IET Commun., vol. 8, no. 9, pp. 1437-1446, June 2014.

[16] T. Kamalakis, I. Neokosmidis, A. Tsipouras, T. Sphicopoulos, S. Pantazis, and I. Andrikopoulos, “Hybrid free space optical/ millimeter wave outdoor links for broadband wireless access networks,” Int. Symp. on Personal, Indoor and Mobile Radio Communication, pp. 1-5, Sept. 2007.

[17] Z. Ghassemlooy, W. Popoola, and S. Rajbhandari, “Visible light communications theory and applications,” CRC press, NY, 2017.

[18] E. Mostafapour, C. Ghobadi, M. Chehel Amirani, “Non-stationary channel estimation with diffusion adaptation strategies over distributed networks,” Wireless Personal Communication, vol. 99, no. 3, pp. 1377-1390, Jan. 2018.

[19] A. Khalili, M.A. Tinati, A. Rastegarnia, and J. A. Chambers, “Steady state analysis of diffusion LMS adaptive networks with noisy links,” IEEE Trans. Signal Process. vol. 60, no. 2, pp. 974-979, Feb. 2012.

[20] M. Uysal, S. Mohammad Navidpour, and J. Li. “Error rate performance of coded free-space optical links over strong turbulence channels,” IEEE Communications Letters, vol. 8, no. 10, pp. 635-637, Oct. 2004.

[21] M. Uysal, L. Jing, and Y. Meng, “Error rate performance analysis of coded free-space optical links over Gamma-Gamma atmospheric turbulence channels,” IEEE Trans. Wireless Commun., vol. 5, no. 6, pp. 1229-1233, June 2006.

[22] E. Mostafapour, Ch. Ghobadi, J. Nourinia, and M. Chehel Amirani, “Tracking performance of incremental LMS algorithm over adaptive distributed sensor network, ” Journal of communication engineering, vol. 4, no. 1, pp. 55-66, Spring 2015.

[23] M. D. Kafiul Islam , A. Rastegarnia, and A. Khalili, “A robust distributed estimation algorithm under Alpha-stable noise condition, ” Journal of communication engineering, vol. 4, no. 2, pp. 76-85, Autumn 2015.

[24] L. Li, J.A. Chambers C. G. Lopez and A. H. Sayed, “Distributed estimation over adaptive incremental network based on affine projection algorithm,” IEEE Trans. Signal Process. vol. 58, no. 1, pp. 151-164, Jan. 2010.